

**The role of climatic
and terrain**

J. L. Peña-Arancibia et al.

This discussion paper is/has been under review for the journal Hydrology and Earth System Sciences (HESS). Please refer to the corresponding final paper in HESS if available.

The role of climatic and terrain attributes in estimating baseflow recession in tropical catchments

J. L. Peña-Arancibia^{1,2,3}, A. I. J. M. van Dijk³, M. Mulligan¹, and L. A. Bruijnzeel²

¹Environmental Monitoring and Modelling Research Group, Department of Geography, King's College London, Strand, London WC2R 2LS, UK

²Faculty of Earth and Life Sciences, VU University Amsterdam, De Boelelaan 1085–1087, 1081 HV, Amsterdam, The Netherlands

³CSIRO Land and Water, GPO 1666, Black Mountain ACT, Canberra, Australia

Received: 13 June 2010 – Accepted: 14 June 2010 – Published: 1 July 2010

Correspondence to: J. L. Peña-Arancibia (jorge.pena_arancibia@kcl.ac.uk)

Published by Copernicus Publications on behalf of the European Geosciences Union.

Title Page	
Abstract	Introduction
Conclusions	References
Tables	Figures
◀	▶
◀	▶
Back	Close
Full Screen / Esc	
Printer-friendly Version	
Interactive Discussion	



Abstract

The understanding of low flows in rivers is paramount more than ever as demand for water increases on a global scale. At the same time, limited streamflow data to investigate this phenomenon, particularly in the tropics, makes the provision of accurate estimations in ungauged areas an ongoing research need. This paper analysed the potential of climatic and terrain attributes of 167 tropical and sub-tropical unregulated catchments to predict baseflow recession rates. Climatic attributes included annual and seasonal indicators of rainfall and potential evapotranspiration. Terrain attributes included indicators of catchment shape, morphology, land cover, soils and geology. Stepwise regression was used to identify the best predictors for baseflow recession coefficients (k_{bf}). Mean annual rainfall (MAR) and aridity index (AI) were found to explain 49% of the spatial variation of k_{bf} . The rest of climatic indices plus average catchment slope (SLO) and tree cover were also good predictors, but co-correlated with MAR. Catchment elongation (CE), a measure of catchment shape, was also found to be statistically significant, although weakly correlated. An analysis of clusters of catchments of smaller size, showed that in these areas, presumably with some similarity of soils and geology due to proximity, residuals of the regression could be explained by SLO and CE. The approach used provides a potential alternative for k_{bf} parameterisation in ungauged areas.

1 Introduction

The gradual depletion of water stored in a catchment during dry weather constitutes the drainage or baseflow recession (Tallaksen, 1995). The understanding of quantities and temporal patterns of baseflow are central to water resources management, particularly in catchments with marked streamflow seasonality (Vogel and Kroll, 1992; Bruijnzeel, 2004; Brandes et al., 2005).

HESSD

7, 4059–4087, 2010

The role of climatic and terrain

J. L. Peña-Arancibia et al.

Title Page

Abstract

Introduction

Conclusions

References

Tables

Figures

◀

▶

◀

▶

Back

Close

Full Screen / Esc

Printer-friendly Version

Interactive Discussion



The role of climatic and terrain

J. L. Peña-Arancibia et al.

[Title Page](#)[Abstract](#)[Introduction](#)[Conclusions](#)[References](#)[Tables](#)[Figures](#)[I◀](#)[▶I](#)[◀](#)[▶](#)[Back](#)[Close](#)[Full Screen / Esc](#)[Printer-friendly Version](#)[Interactive Discussion](#)

In recent years, several assessments of global water resources have been conducted using hydrological models and land surface models (LSMs); mainly in response to increase in water demand and potential impacts of climatic and land use change (Vörösmarty et al., 2000; Oki and Kanae, 2006). Linear conceptual storage-discharge models have been used to simulate baseflow recession in many of these models. Although some hydrological processes may lead to a non-linear behaviour; research indicates that low flows during dry periods can be adequately approximated by linear reservoirs (Zecharias and Brutsaert, 1988; Vogel and Kroll, 1992; Chapman, 1999; Fenicia et al., 2006, Van Dijk, 2010).

In many cases, the linear reservoir application in global hydrological models used fixed parameter values, e.g. the routing HD model (Hagemann and Dümenil 1998), macro-PDM (Arnell, 1999, 2003) and WGHM (Döll et al., 2003). Inferred values from drainage theory have been used in PCR-GLOBWB (Van Beek and Bierkens, 2008) whereas calibrated values were used in the global application of WASMOD-M (Widen-Nilsson et al., 2007) and in an application of the Catchment Land Surface Model (CLSM) to the Somme River Basin (Gascoïn et al., 2009). The use of drainage theory (e.g., Brutsaert and Nieber, 1977) is questionable at large scales and is also hindered by the uncertain quality of data needed to estimate various subsurface parameters. Also, the density of streamflow station data – used on a routine basis to calibrate conceptual models – is not spatially uniform, particularly in remote forested areas. Moreover, calibration approaches are not practical for global application because of the large number of locations for which separate calibrations would be needed (Nijssen et al., 2001). Nijssen et al. (2001) modelled the seasonal discharge of 26 large basins in the world (including the Amazon, Congo and Mekong). Data from the Global River Discharge Center (GRDC) in Koblenz-Germany were used to parameterise the conceptual quasi-linear baseflow reservoir component of the VIC model (Liang et al., 1994). Baseflow recession coefficients (k_{br}) were determined for 347 stations that had good quality data using a linear regression on the log-transformed discharges and then interpolated to the nearest areas.

The role of climatic and terrain

J. L. Peña-Arancibia et al.

Title Page

Abstract

Introduction

Conclusions

References

Tables

Figures

◀

▶

◀

▶

Back

Close

Full Screen / Esc

Printer-friendly Version

Interactive Discussion



On the other hand, several studies have correlated terrain attributes – including catchment morphology and soil type – to estimate k_{bf} in different climatic and physiographic regions or for geological formations across the world (e.g., Post and Jake-
 5 man, 1996; Yu et al., 2002; Brandes et al., 2005). Most studies have focused on small catchments ($<200 \text{ km}^2$) located in common physiographic regions of similar climate. Van Dijk (2010) included climatic attributes in addition to terrain attributes to analyse the relationship with k_{bf} for 183 mainly temperate Australian catchments. The results showed that baseflow recession from a linear reservoir was best explained by climatic
 10 attributes, with catchment aridity index (AI, the ratio of rainfall to potential evapotranspiration) explaining 27% of the variation in derived recession coefficients. No correlations were found with catchment morphology or geology; however, spatial coherence of the residual unexplained variation showed that another 53% of the variation was spatially correlated over distances of 100–150 km. This was probably associated with terrain factors not captured by the available data and the large geographical spread of individ-
 15 ual catchments (Van Dijk, 2010).

Motivated by the latter results, the objective of the present study is to identify the dominant climatic and terrain attributes that control the variance of k_{bf} in tropical and sub-tropical catchments. There is a dearth of studies that have investigated these relationships in the tropics and most of them were limited to small geographic regions
 20 (e.g., Yu et al., 2002; Mwakalila et al., 2002).

Subsidiary goals are to: (i) to assemble a dataset of good quality streamflow gauge data for tropical catchments and to obtain the associated climatic and terrain attributes; and (ii) build equations based on the parameters that best explain k_{bf} in gauged catch-
 25 ments to estimate this parameter for ungauged catchments. The relationships derived can be potentially used by the aforementioned global scale hydrology models to provide an estimate of k_{bf} in ungauged tropical catchments.

2 Theory

Good literature reviews on baseflows and recession analysis are provided by Tallaksen (1995), Wittenberg (1999) and Smakhtin (2001). In this paper, only a summary of the rationale and the main equations involved in baseflow recession analysis are presented. The theoretical framework of this study follows the one presented in Van Dijk (2010).

A linear reservoir model requires a recession coefficient (k_{bf}) to separate daily streamflow data into baseflow and quickflow and is expressed as:

$$Q_{bf} = -k_{bf}S \quad (1)$$

where Q_{bf} (in mm day^{-1}) is the flow rate during the baseflow recession period, S (mm) is reservoir storage. The constant k_{bf} is expressed in day^{-1} .

Streamflow data representative of baseflow needs not to be affected by stormflow (QF). It is assumed that stormflow affects streamflow for a period of T_{QF} days after the event peak flow (Van Dijk, 2010). Van Dijk (2010) found that for catchments in Australia, the number of data pairs decreased exponentially with increasing T_{QF} period. Vogel and Kroll (1992) considered baseflow recession to start when the 3-day streamflow moving average begins to decrease, and the recession to end when the 3-day moving average start to increase. A period of 5 days (T_{QF5}) was considered a useful compromise between representative low flow conditions and data availability. Increasing the window size to more days would have resulted in many catchments being dropped from the analysis. This criterium was considered to construct Q and Q^* (Q of the previous day) data pairs representative of baseflow conditions for each gauging station. All days with zero streamflow and or missing data were also excluded. By using a representative number of $Q-Q^*$ data pairs it is possible to estimate the recession coefficient k_{bf} , this will be described further on.

The role of climatic and terrain

J. L. Peña-Arancibia et al.

Title Page

Abstract

Introduction

Conclusions

References

Tables

Figures

◀

▶

◀

▶

Back

Close

Full Screen / Esc

Printer-friendly Version

Interactive Discussion



analysis of frequency distributions for k_{bf} and various climatic indices and catchment attributes was conducted to assess applicable correlations methods. Furthermore, a non-parametric correlation matrix was used to determine the degree of correlation between recession constants and catchment attributes. Finally, predictive relationships were obtained using stepwise regression. Figure 1 presents a summary flowchart of the procedure described above.

3.1 Climatic and terrain attributes of pan-tropical catchments

Several climatic and terrain attributes with a demonstrated correlation with baseflow parameters (e.g., Post and Jakeman, 1996; Brandes et al., 2005; Van Dijk, 2010) were derived for each catchment. A summary of parameters, their original resolution and source are summarised in Table 1. Climatic attributes included annual and seasonal descriptors of rainfall and potential evapotranspiration and were defined as follows:

- Mean annual rainfall (MAR) expressed in mm y^{-1} obtained from the WORLDCLIM dataset (Hijmans et al., 2005).
- Potential evapotranspiration (PET) in mm y^{-1} estimated using the Hargreaves et al. (1985) model formulation and parameterised as described in Trabucco et al. (2008).
- Aridity index ($\text{AI}=\text{MAR}/\text{PET}$).
- Thornthwaite Moisture Index (TMI, Thornthwaite, 1948). An overall measure of precipitation effectiveness on a monthly basis. It is estimated using monthly

The role of climatic and terrain

J. L. Peña-Arancibia et al.

Title Page

Abstract

Introduction

Conclusions

References

Tables

Figures

◀

▶

◀

▶

Back

Close

Full Screen / Esc

Printer-friendly Version

Interactive Discussion



rainfall and PET totals from the above mentioned datasets as follows:

$$TMI = \frac{\sum_{m=1}^{12} (100s_m - 60d_m)}{PET} \quad (4)$$

where s is the monthly water surplus and d is the monthly water deficit (mm mo^{-1}).

- 5 – Seasonality index. The seasonality index (SI, Walsh and Lawler, 1981) is defined as the sum of the absolute deviation of mean monthly rainfall ($\overline{X_m}$) from the overall monthly mean divided by the mean annual rainfall (MAR):

$$SI = \frac{1}{MAR} \sum_{m=1}^{12} \left| \overline{X_m} - \frac{MAR}{12} \right| \quad (5)$$

10 The SI varies from zero (when all months have the same rainfall) to 1.83 (when all rainfall occurs in a single month): values <0.19 indicate a very equable rainfall regime, whereas values between 0.20 and 0.99 indicate a seasonal rainfall regime and values >1 a short wet season.

Terrain attributes included indicators of catchment shape, morphology, land cover, soils and geology.

- 15 – Catchment shape, defined by catchment elongation (CE) in km^2 surface area per km of catchment length, or by the ratio of a circle with the same area as the catchment to the catchment's length (Post and Jakeman, 1996).
- 20 – Mean catchment rainfall weighted slope (SLO) (%). To account for spatial variability in rainfall, each catchment slope pixel is scaled using normalised mean catchment rainfall data.

The role of climatic and terrain

J. L. Peña-Arancibia et al.

Title Page

Abstract

Introduction

Conclusions

References

Tables

Figures

◀

▶

◀

▶

Back

Close

Full Screen / Esc

Printer-friendly Version

Interactive Discussion



formulation gives equal weighting to all data pairs however weighting influence by very low or very large values when using different objective functions cannot be entirely avoided.

3.3 Statistical analysis

5 A correlation matrix was used to determine the correlation between various catchment attributes and the recession coefficients. The attributes with the best individual explanatory values were combined into a stepwise multiple regression equation. Exponential, logarithmic and power functions were computed to link potential predictors to k_{bf} , and the best regression was selected to subsequently predict k_{bf} . Attributes
10 that co-correlated were not considered in the subsequent stepwise regression. After selecting the best equation, the same types of regression were computed for both the absolute and relative residual variance and the remaining potential predictors, until no further variation was explained by adding these.

4 Results

15 4.1 Assembling a pan-tropical dataset for baseflow modelling

Catchment boundaries were obtained from the Hydrosheds 1 km river network (Lehner et al., 2010). Only catchments with a relative error of less than 10% between the GRDC reported surface areas and the river network derived areas were considered in the analysis. After controlling for regulation, snow and lake influence and land use
20 change; the analysis resulted in a database comprising 167 catchments worldwide (Fig. 2a). Of the 167 catchments 50% had a catchment area $<1000 \text{ km}^2$ and 90% $<6000 \text{ km}^2$.

The catchment assemblage showed good spatial coverage, encompassing many tropical climates (Fig. 2b). A large number of stream gauging stations were located in
25 Australia. No stations complying with the aforementioned requirements were found in

The role of climatic and terrain

J. L. Peña-Arancibia et al.

Title Page

Abstract

Introduction

Conclusions

References

Tables

Figures

◀

▶

◀

▶

Back

Close

Full Screen / Esc

Printer-friendly Version

Interactive Discussion



the Amazon or Congo Basins. Most stations in the latter basins had monthly records or short daily records, which excluded them from the present analysis of daily flows.

4.2 Estimation of recession coefficient k_{bf}

The overall mean k_{bf} for the 167 analysed catchments was of 0.08 ± 0.053 (std. dev.) day^{-1} . The distribution was positively skewed. Higher values were found in arid catchments and lower values in wetter catchments. In addition, lower values were generally found in catchment closer to the coastline.

In Australia, the lowest values of k_{bf} ($0.02\text{--}0.08 \text{ day}^{-1}$) were generally found in catchments that lie closer to the east and north coastlines. Catchments located in the more arid interior had values of $0.11\text{--}0.18 \text{ day}^{-1}$. In Southeast Asia, the fully humid Malayan Peninsula had values of $0.02\text{--}0.06 \text{ day}^{-1}$. Continental Southeast Asia showed values of $0.04\text{--}0.07 \text{ day}^{-1}$. The highest values in Africa were found in Namibia (0.20 day^{-1}) and in the catchments located in the northernmost of the Sahel (0.17 day^{-1}). Catchments located closer to the coastline in West Africa and Central Africa (Congo and Zambia) generally showed values of $\sim 0.035 \text{ day}^{-1}$, as did temperate catchments in South Africa. Catchments located in the Andes had values of $0.03\text{--}0.08 \text{ day}^{-1}$. Catchments in Panama, Costa Rica Nicaragua and Honduras had mostly values around $0.03\text{--}0.09 \text{ day}^{-1}$ whereas catchments in Puerto Rico had values of 0.05 day^{-1} . In tropical Mexico, catchments close to the coastline had values of $0.03\text{--}0.10 \text{ day}^{-1}$.

4.3 Statistical analyses

Visual inspection of scatter plots (Fig. 3) already suggested catchment recession coefficients to be correlated to various climatic attributes. Of the respective terrain attributes, only slope and tree cover appeared to show some correlation (Fig. 3). The rest of the catchment attributes did not reveal a clear pattern (not shown). In addition, different aquifer drainage potential classes did not seem to have any influence on k_{bf} either (Fig. 3).

The role of climatic and terrain

J. L. Peña-Arancibia et al.

Title Page

Abstract

Introduction

Conclusions

References

Tables

Figures

◀

▶

◀

▶

Back

Close

Full Screen / Esc

Printer-friendly Version

Interactive Discussion



The role of climatic and terrain

J. L. Peña-Arancibia et al.

Title Page

Abstract

Introduction

Conclusions

References

Tables

Figures

◀

▶

◀

▶

Back

Close

Full Screen / Esc

Printer-friendly Version

Interactive Discussion



Recession coefficient data showed a positively skewed distribution and thus a non-parametric Spearman rho test was used in the correlation analysis. The correlation matrix is presented in Table 2. Significant strong correlations were found between k_{bf} and most climatic attributes; slope and tree cover. As expected, cross-correlations occurred between all climatic attributes. In addition, cross-correlations between slope, tree cover and climatic attributes were also observed. A relationship between tree cover, catchment slope and MAR is also intuitively possible, for instance in the case of steep mountainous terrain where difficulty of access increases the chances of forest conservation and topography and altitude lead to enhanced orographic rainfall. The best correlations for k_{bf} were with MAR and the Thornthwaite Moisture Index TMI (non-parametric $r^* = -0.65$). AI also showed good correlation with k_{bf} ($r^* = -0.64$). Regression equations were computed for k_{bf} vs. MAR and AI, results are shown in Fig. 4 (no power or exponential regression were possible for negative values of TMI).

A two-parameter exponential relationship of MAR and AI explained 49% of the variance in k_{bf} . Only marginal improvement was achieved with the stepwise regression when including the weakly correlated catchment elongation (CE, $r^* = 0.138$). The other catchment terrain attributes with explanatory value were cross-correlated to climatic attributes and therefore not used in the multivariate analysis. The equations and summary statistics of all regressions are shown in Table 3.

A subset of catchments that were smaller and geographically close to each other, contiguous in some cases, were analysed to see whether the correlation of catchment terrain properties with k_{bf} was confounded by the large geographical area and the different climates covered by the overall dataset (cf. Fig. 2a). Relatively smaller groups of catchments ($<300 \text{ km}^2$) were selected in north, central and south Queensland and in Puerto Rico. Only clusters of larger catchments ($500\text{--}3000 \text{ km}^2$) were left for analysis and so they were selected in the absence of data more suited to the purpose, in any case only two catchments were larger than 1500 km^2 . These were located in Panama, Senegal and Malaysia. Relative residuals of the original regression of k_{bf} and MAR were analysed using scatter plots and non-parametric correlation. Only slope and

catchment elongation showed significant correlations ($r^*=350$ and -250 , respectively). Although correlations were weak, scatter plots of such properties versus relative residuals showed some degree of spatial organisation by location (Fig. 5).

5 Discussion

5.1 Pan tropical catchment dataset

In the present study, great care was taken in producing a good quality daily streamflow dataset of unregulated flows (using the georeferenced dam dataset of Saenz and Mulligan) for tropical landscapes. A good range of climatic landscapes and rainfall regimes has been covered, but data from hydrologically important areas such as the Amazon and Congo basins are not yet represented in the analysis. Needless to say, their inclusion is highly desirable.

5.2 Characteristics of recession coefficients

In general, higher (faster) recession coefficients were observed for drier and flatter catchments. In the most arid catchments (e.g., Namibia, arid parts of Australia) streamflow is typically ephemeral and consequently mainly event driven. The presence of fast-draining perched aquifers may also explain higher k_{bf} . By contrast, lower recession coefficients (slower drainage) were found for most of the humid tropics. Although there were no good quality data to account for the effects of soil depth and aquifer porosity, deep soils and permeable regoliths are widely present in tropical landscapes; and are likely to represent an important source of baseflow (Chappell et al., 2007). A recent three-year study in a small catchment underlain by very deep soils in the central Amazon Basin by Tomasella et al. (2008) showed an important contribution to the groundwater system by the extended unsaturated zone. Both unsaturated and groundwater flow showed a delayed response to rainfall and most of the seasonal variability in streamflow tended to be dampened by either one or the other.

The role of climatic and terrain

J. L. Peña-Arancibia et al.

Title Page

Abstract

Introduction

Conclusions

References

Tables

Figures

◀

▶

◀

▶

Back

Close

Full Screen / Esc

Printer-friendly Version

Interactive Discussion



5.3 Predictors of recession coefficients

Climatic attributes proved to be the best predictors of k_{bf} , with MAR and AI together explaining 49% of the variance. The exponential and logarithmic regression equations for AI and MAR had very similar goodness-of-fit statistics but due to the nature of the fitted equations estimation errors appeared higher for drier catchments in all equations (cf. Fig. 4). For wetter catchments, both logarithmic and power relations approached the asymptotic value of 0.05 too gradually. The robustness of the equations for MAR and AI intervals was checked using box and whisker plots of relative residuals for all equations. The exponential equations for MAR and AI were slightly more robust than the other equations for all intervals, and MAR was only marginally better than AI (Fig. 6).

Pan-tropical maps of k_{bf} extending to 30° N and 35° S were derived using the MAR regression equation and the lower and upper bounds of the 95% confidence interval. The resulting catchment k_{bf} values are plotted in the map showing the original value (Fig. 7).

The analysis of relative residuals for smaller catchments showed that catchment attributes such as slope (SLO) and elongation ratio (CE) had weak correlations with k_{bf} . Studies in catchments <100 km² (e.g., Post and Jakeman, 1996; Brandes et al., 2005) also showed the explanatory power of terrain attributes and soils with respect to k_{bf} or other baseflow associated parameters. The present study and Van Dijk (2010) have demonstrated a similar importance of climate characteristics in relation to baseflow recessions across the tropics and Australia. Van Dijk (2010, Fig. 7 for the AI vs. k_{bf} plot) obtained similar power relationships between MAR, AI and baseflow recessions respectively for temperate Australian catchments. Estimates of k_{bf} using the equations derived in the present study produced slightly higher estimates in these catchments, but the form of the relationships were similar. Differences between the rainfall data, and the Priestley-Taylor PET formulation in Van Dijk (2010) with the Hargreaves formulation in the present study may explain these differences.

The role of climatic and terrain

J. L. Peña-Arancibia et al.

Title Page

Abstract

Introduction

Conclusions

References

Tables

Figures

◀

▶

◀

▶

Back

Close

Full Screen / Esc

Printer-friendly Version

Interactive Discussion



catchment shape, morphology, land cover, soils and geology. Stepwise regression showed the best predictors for baseflow recession coefficient (k_{bf}) were mean annual rainfall (MAR) and aridity index (AI) together explaining 49% of the variance. Catchment elongation (CE), a measure of catchment shape, was also found to be statistically significant, although weakly correlated. An analysis of clusters of catchments of smaller size, showed that in these areas with presumably similar soils and geology, residuals of the regression could be explained by average catchment slope (SLO) and CE.

Ephemeral and consequently mainly event-driven streamflow as well as the occurrence of fast-draining perched aquifers may explain the higher recession coefficients observed in drier and flatter catchments. The lowest recession coefficients in the humid tropics may be attributed to excess rainfall recharging deep soils and porous aquifers present in these areas (e.g., volcanic belts Central Amazonia, sandstone basin forms in Northeast Thailand). These sources may be an important source of baseflow during dry weather.

Although some climatic characteristics explained a great deal of the variation in k_{bf} , baseflow is catchment-specific and dependent on the rainfall spatial and temporal patterns, land cover and land use, catchment morphology, infiltration opportunities and soil water holding capacity, configuration of the groundwater system and timing of groundwater discharge to the stream. If better data are obtained for these surface and subsurface attributes, the prediction of baseflow in ungauged areas can be improved accordingly.

Acknowledgements. The authors gratefully acknowledge the funding from Microsoft Research and the Basin Focal Project Andes, a project of the CGIAR Challenge Program on Water and Food (CPWF). The GRDC Runoff Data Center and Francis Chiew of CSIRO Land and Water are also thanked for providing the streamflow data. The authors are also grateful to Hannah Cloke from King's College London for providing valuable comments on the research. This study was conducted during an internship carried on in CSIRO Land and Water, Canberra-Australia and is part of the PhD dissertation of the first author.

The role of climatic and terrain

J. L. Peña-Arancibia et al.

Title Page

Abstract

Introduction

Conclusions

References

Tables

Figures

◀

▶

◀

▶

Back

Close

Full Screen / Esc

Printer-friendly Version

Interactive Discussion



References

- Arino, O., Bicheron, P., Achard, F., Latham, J., Witt, R., and Weber, J. L.: GLOBCOVER The most detailed portrait of Earth, Esa Bulletin-European Space Agency, 24–31, 2008.
- 5 Arnell, N. W.: A simple water balance model for the simulation of streamflow over a large geographic domain, *J. Hydrol.*, 217, 314–335, 1999.
- Arnell, N. W.: Effects of IPCC SRES* emissions scenarios on river runoff: a global perspective, *Hydrol. Earth Syst. Sci.*, 7, 619–641, doi:10.5194/hess-7-619-2003, 2003.
- 10 Batjes, N. H.: ISRIC-WISE derived soil properties on a 5 by 5 arc-minutes global grid (version 1.0). Report 2006/02 ISRIC World Soil Information, Wageningen 2006, available at: http://www.isric.org/isric/webdocs/Docs/ISRIC_Report.2006.02.pdf, data available at: <http://www.isric.org>, last access: 17 May 2010.
- Brandes, D., Hoffmann, J. G., and Mangarillo, J. T.: Base flow recession rates, low flows, and hydrologic features of small watersheds in Pennsylvania, USA, *J. Am. Water Resour. As.*, 41, 1177–1186, 2005.
- 15 Bruijnzeel, L. A.: Hydrological functions of tropical forests: not seeing the soil for the trees?, *Agr. Ecosyst. Environ.*, 104, 185–228, doi:10.1016/j.agee.2004.01.015, 2004.
- Brutsaert, W. and Nieber, J. L.: Regionalized drought flow hydrographs from a mature glaciated plateau, *Water Resour. Res.*, 13, 637–644, 1977.
- Chapman, T.: A comparison of algorithms for stream flow recession and baseflow separation, *Hydrol. Process.* 13, 601–604, 1999.
- 20 Chappell, N. A., Sherlock, M., Bidin, K., Macdonald, R., Najman, Y., and Davies, G.: Runoff processes in Southeast Asia: role of soil, regolith, and rock type, *Forest Environments in the Mekong River Basin*, 3–23, 2007.
- Defries, R. S., Hansen, M. C., Townshend, J. R. G., Janetos, A. C., and Loveland, T. R.: A new global 1-km dataset of percentage tree cover derived from remote sensing, *Glob. Change Biol.*, 6, 247–254, 2000.
- 25 Doll, P., Kaspar, F., and Lehner, B.: A global hydrological model for deriving water availability indicators: model tuning and validation, *J. Hydrol.*, 270, 105–134, 2003.
- Fenicia, F., Savenije, H. H. G., Matgen, P., and Pfister, L.: Is the groundwater reservoir linear? Learning from data in hydrological modelling, *Hydrol. Earth Syst. Sci.*, 10, 139–150, doi:10.5194/hess-10-139-2006, 2006.
- 30

The role of climatic and terrain

J. L. Peña-Arancibia et al.

Title Page

Abstract

Introduction

Conclusions

References

Tables

Figures

◀

▶

◀

▶

Back

Close

Full Screen / Esc

Printer-friendly Version

Interactive Discussion



The role of climatic and terrainJ. L. Peña-Arancibia et al.

[Title Page](#)[Abstract](#)[Introduction](#)[Conclusions](#)[References](#)[Tables](#)[Figures](#)[◀](#)[▶](#)[◀](#)[▶](#)[Back](#)[Close](#)[Full Screen / Esc](#)[Printer-friendly Version](#)[Interactive Discussion](#)

- Gascoïn, S., Ducharne, A., Ribstein, P., Carli, M., and Habets, F.: Adaptation of a catchment-based land surface model to the hydrogeological setting of the Somme River Basin (France), *J. Hydrol.*, 308, 105–116, 2009.
- 5 Hagemann, S. and Dumenil, L.: A parametrization of the lateral waterflow for the global scale, *Clim. Dynam.*, 14, 17–31, 1998.
- Hijmans, R. J., Cameron, S. E., Parra, J. L., Jones, P. G., and Jarvis, A.: Very high resolution interpolated climate surfaces for global land areas, *Int. J. Climatol.*, 25, 1965–1978, doi:10.1002/joc.1276, 2005.
- 10 Lehner, B., Verdin, K., and Jarvis, A.: Hydrosheds technical documentation, Version 1.1, data available at: <http://hydrosheds.cr.usgs.gov> (last access 17 May 2010), 2008.
- Lepers, E., Lambin, E. F., Janetos, A. C., DeFries, R., Achard, F., Ramankutty, N., and Scholes, R. J.: A synthesis of information on rapid land-cover change for the period 1981–2000, *Bioscience*, 55, 115–124, 2005.
- 15 Liang, X., Lettenmaier, D. P., Wood, E. F., and Burges, S. J.: A simple hydrologically based model of land-surface water and energy fluxes for general-circulation models, *J. Geophys. Res.-Atmos.* 99, 14415–14428, 1994.
- Mwakalila, S., Feyen, J., and Wyseure, G.: The influence of physical catchment properties on baseflow in semi-arid environments, *J. Arid Environ.*, 52, 245–258, doi:10.1006/jare.2001.0947, 2002.
- 20 Nijssen, B., O'Donnell, G. M., Lettenmaier, D. P., Lohmann, D., and Wood, E. F.: Predicting the discharge of global rivers, *J. Climate*, 14, 3307–3323, 2001.
- Oki, T. and Kanae, S.: Global hydrological cycles and world water resources, *Science*, 313, 1068–1072, doi:10.1126/science.1128845, 2006.
- Post, D. A. and Jakeman, A. J.: Relationships between catchment attributes and hydrological response characteristics in small Australian mountain ash catchments, *Hydrol. Process.*, 10, 877–892, 1996.
- 25 Saenz, L. and Mulligan, M.: Development and validation of a georeferenced tropics-wide database of dams, *Water Resour. Res.*, to be submitted, 2010.
- Smakhtin, V. U.: Low flow hydrology: a review, *J. Hydrol.*, 240, 147–186, 2001.
- 30 Tallaksen, L. M.: A review of baseflow recession analysis, *J. Hydrol.*, 165, 349–370, 1995.
- Thornthwaite, C. W.: An approach toward a rational classification of climate, *Geogr. Rev.*, 38, 55–94, 1948.

Tomasella, J., Hodnett, M. G., Cuartas, L. A., Nobre, A. D., Waterloo, M. J., and Oliveira, S. M.: The water balance of an Amazonian micro-catchment: the effect of interannual variability of rainfall on hydrological behaviour, *Hydrol. Process.*, 22, 2133–2147, doi:10.1002/hyp.6813, 2008.

5 Van Beek, L. P. H. and Bierkens, M. F. P.: The Global Hydrological Model PCR-GLOBWB: Conceptualization, Parameterization and Verification, 2008. Report Department of Physical Geography, Utrecht University, Utrecht, The Netherlands, available at: <http://vanbeek.geo.uu.nl/suppinfo/vanbeekbierkens2009.pdf>, last access: 17 May 2010.

10 van Dijk, A. I. J. M.: Climate and terrain factors explaining streamflow response and recession in Australian catchments, *Hydrol. Earth Syst. Sci.*, 14, 159–169, doi:10.5194/hess-14-159-2010, 2010.

Vogel, R. M. and Kroll, C. N.: Regional geohydrologic-geomorphic relationships for the estimation of low-flow statistics, *Water Resour. Res.*, 28, 2451–2458, 1992.

15 Vorosmarty, C. J., Green, P., Salisbury, J., and Lammers, R. B.: Global water resources: vulnerability from climate change acid population growth, *Science*, 289, 284–288, 2000.

Walsh, R. P. D. and Lawler, D. M.: Rainfall seasonality: description, spatial patterns and change through time, *Weather*, 36, 201–209, 1981.

20 WHYMAP – World-wide Hydrogeological Mapping and Assessment Programme, Groundwater resources of the world, 2010, data available at: <http://www.bgr.de/app/fishy/GoogleEarth/whymap.kml>, last access 17 May 2010.

Widen-Nilsson, E., Halldin, S., and Xu, C. Y.: Global water-balance modelling with WASMOD-M: parameter estimation and regionalisation, *J. Hydrol.*, 340, 105–118, doi:10.1016/j.jhydrol.2007.04.002, 2007.

25 Wittenberg, H.: Baseflow recession and recharge as nonlinear storage processes, *Hydrol. Process.*, 13, 715–726, 1999.

Yu, P. S., Yang, T. C., and Liu, C. W.: A regional model of low flow for Southern Taiwan, *Hydrol. Process.*, 16, 2017–2034, 2002.

30 Zecharias, Y. B. and Brutsaert, W.: Recession characteristics of groundwater outflow and baseflow from mountainous watersheds, *Water Resour. Res.*, 24, 1651–1658, 1988.

The role of climatic and terrain

J. L. Peña-Arancibia et al.

Title Page

Abstract

Introduction

Conclusions

References

Tables

Figures

◀

▶

◀

▶

Back

Close

Full Screen / Esc

Printer-friendly Version

Interactive Discussion



Table 1. Summary of climatic and terrain attributes used in the present study.

Parameter	Resolution		Source
	Temporal	Spatial	
MAE (mm y ⁻¹)	Monthly average climatology 1950–2000	1 × 1 km grid	WORLDCLIM (Hijmans et al., 2005)
PET (mm y ⁻¹)	Monthly average climatology 1950–2000	1 × 1 km grid	Trabucco et al. (2008; available at http://www.csi.cgiar.org)
AI	NA	1 × 1 km grid	Calculated from MAE and PET
TMI	NA	1 × 1 km grid	Calculated from monthly rainfall and monthly PET
SI	NA	1 × 1 km grid	Calculated from monthly rainfall
CE (m ² m ⁻¹)	NA	NA	Hydrosheds 1 km DEM (Lehner et al., 2010)
SLO (%)	NA	90×90 m grid	Hydrosheds 90 m DEM (Lehner et al., 2010)
DD (km km ⁻²)	NA	90×90 m grid	Hydrosheds 90 m river network available at http://hydrosheds.cr.usgs.gov/hydro.php
TC (%)	NA	1 × 1 km grid	AVHRR Tree Cover Continuous fields (DeFries et al., 2000; available at http://glcf.umd.edu/data/treecover/data.shtml)
SDI	NA	9×9 km grid	ISRIC-WISE derived soil properties (Batjes, 2006)
DPI	NA	NA	WHYMAP (2010)

The role of climatic and terrain

J. L. Peña-Arancibia et al.

Title Page

Abstract

Introduction

Conclusions

References

Tables

Figures

◀

▶

◀

▶

Back

Close

Full Screen / Esc

Printer-friendly Version

Interactive Discussion



The role of climatic and terrain

J. L. Peña-Arancibia et al.

Table 2. Spearman rank correlation matrix of recession coefficients and catchment attributes. k_{bf} correlations with climatic and catchment attributes are shown in bold.

k_{bf}	MAR	PET	AI	TMI	SI	CE	SLO	DD	TC	SD
k_{bf}										
MAR	-0.650**									
PET	0.291**	-0.453**								
AI	-0.639**	0.979**	-0.608**							
TMI	-0.649**	0.987**	-0.564**	0.996**						
SI	0.170*	-0.436**	0.649**	-0.534**	-0.469**					
CE	0.138*	0.119	-0.068	0.105	0.108	0.008				
SLO	-0.380**	0.528**	-0.693**	0.613**	0.587**	-0.499**	0.100			
DD	0.016	0.064	-0.210**	0.088	0.086	-0.005	0.027	0.171*		
TC	-0.425**	0.578**	-0.577**	0.636**	0.618**	-0.436**	0.161*	0.592**	0.353**	
SD	0.007	0.003	0.294**	-0.056	-0.019	0.390**	0.064	-0.304**	0.191**	-0.02

* Correlation is significant at the 0.05 level

** Correlation is significant at the 0.01 level.

Title Page

Abstract

Introduction

Conclusions

References

Tables

Figures

◀

▶

◀

▶

Back

Close

Full Screen / Esc

Printer-friendly Version

Interactive Discussion



The role of climatic and terrain

J. L. Peña-Arancibia et al.

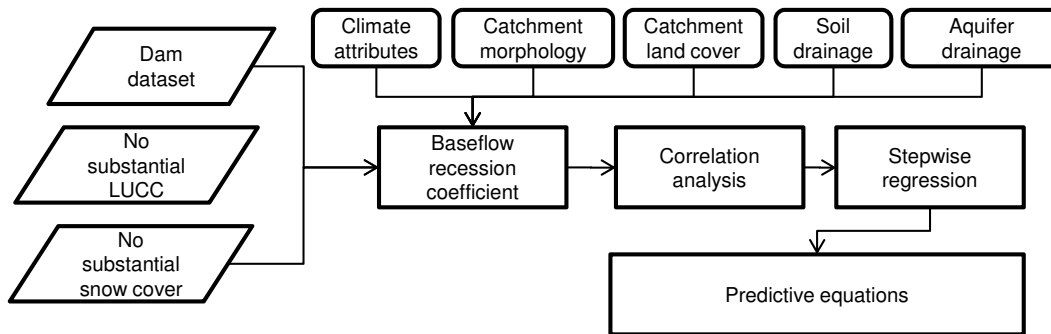


Fig. 1. Methodology flowchart. Unregulated catchments without substantial land use and land cover change (LUCC) and with a snow cover <5% are selected for the analysis. Streamflow had to have at least 5 years of data, 30 runoff events and 30 $Q-Q^*$ data pairs.

Title Page

Abstract

Introduction

Conclusions

References

Tables

Figures

◀

▶

◀

▶

Back

Close

Full Screen / Esc

Printer-friendly Version

Interactive Discussion



The role of climatic and terrain

J. L. Peña-Arancibia et al.

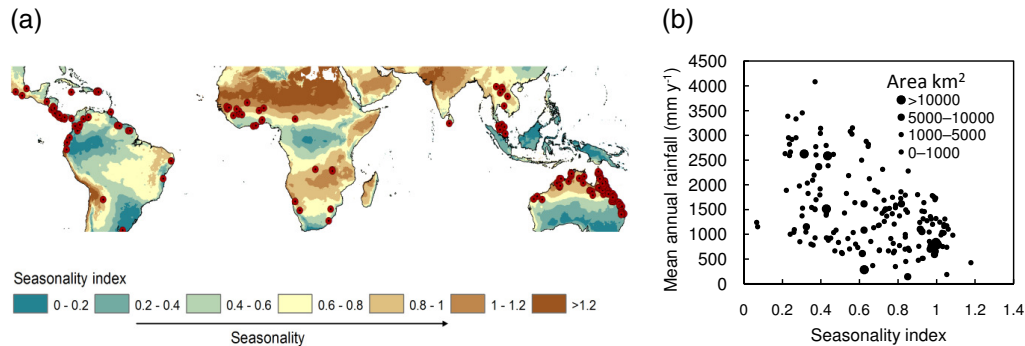


Fig. 2. Distribution of catchments in the dataset: **(a)** Geographic distribution **(b)** in terms of climate using the seasonality index (SI; Walsh and Lowler, 1981). Symbol sizes in **(b)** indicate catchment areas in km².

[Title Page](#)[Abstract](#)[Introduction](#)[Conclusions](#)[References](#)[Tables](#)[Figures](#)[I◀](#)[▶I](#)[◀](#)[▶](#)[Back](#)[Close](#)[Full Screen / Esc](#)[Printer-friendly Version](#)[Interactive Discussion](#)

The role of climatic and terrain

J. L. Peña-Arancibia et al.

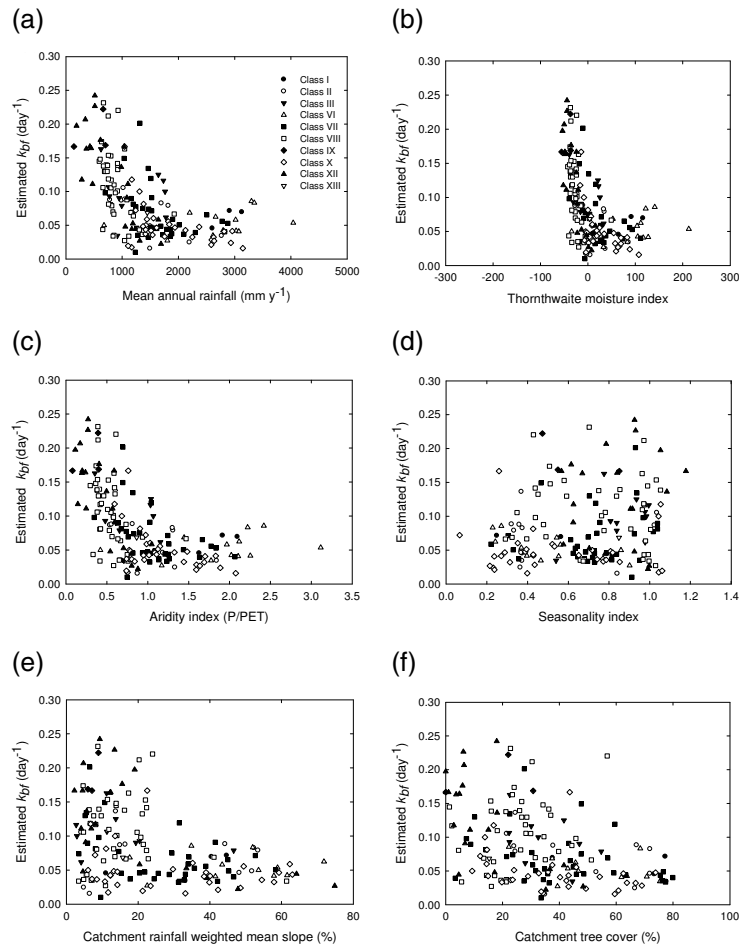


Fig. 3. Scatter plots of recession coefficient k_{bf} versus (a) MAR, (b) TMI, (c) AI, (d) SI, (e) SLO and (f) TC. Symbols denote a proxy for aquifer drainage potential from WHYMAP (2010).

The role of climatic and terrain

J. L. Peña-Arancibia et al.

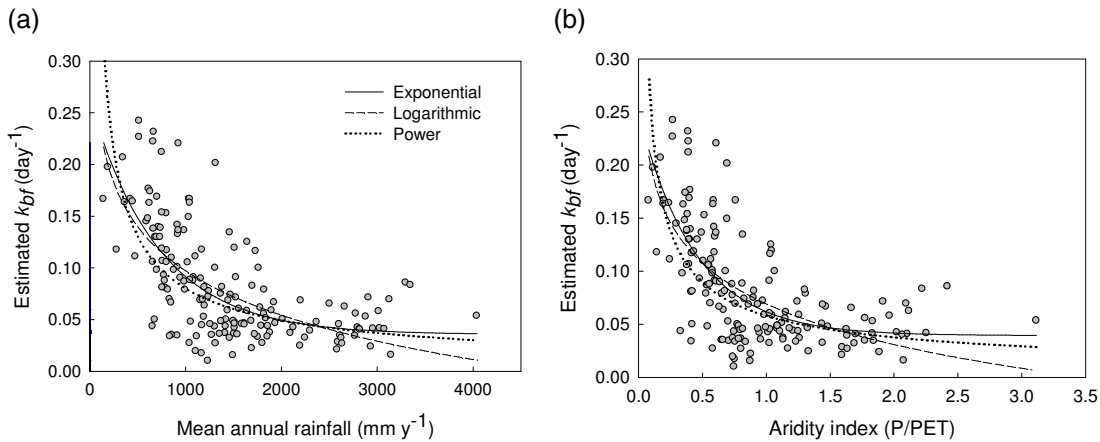


Fig. 4. Regression equations for (a) MAR versus k_{bf} and (b) AI versus k_{bf} .

Title Page

Abstract Introduction

Conclusions References

Tables Figures

◀ ▶

◀ ▶

Back Close

Full Screen / Esc

Printer-friendly Version

Interactive Discussion



The role of climatic and terrain

J. L. Peña-Arancibia et al.

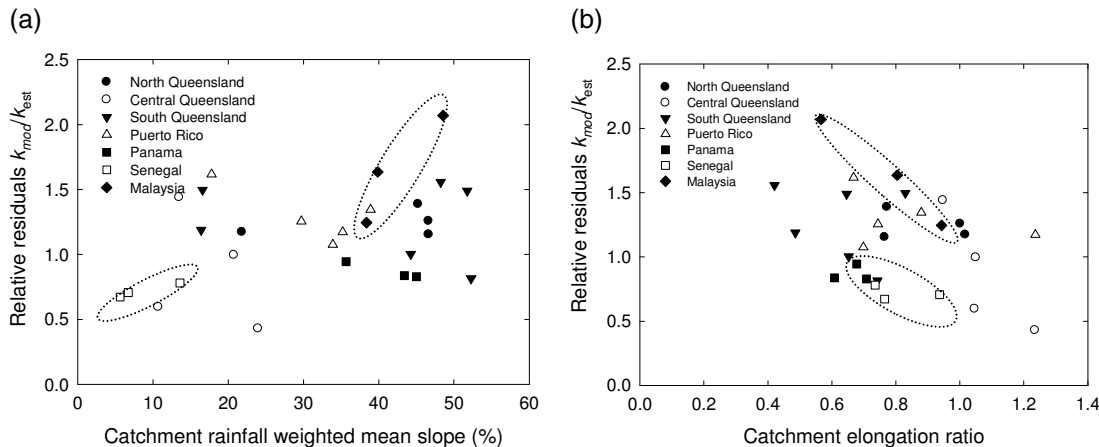


Fig. 5. Scatter plot of relative residuals (ratio of modelled to hydrograph-based estimated k_{bf}) versus **(a)** rainfall weighted slope of catchment (SLO) and **(b)** catchment elongation (CE). Elongated ellipses around Malaysian and Senegal data points are shown to illustrate possible correlations of residuals at smaller scales for geographically close catchments.

Title Page

Abstract

Introduction

Conclusions

References

Tables

Figures

◀

▶

◀

▶

Back

Close

Full Screen / Esc

Printer-friendly Version

Interactive Discussion



The role of climatic and terrain

J. L. Peña-Arancibia et al.

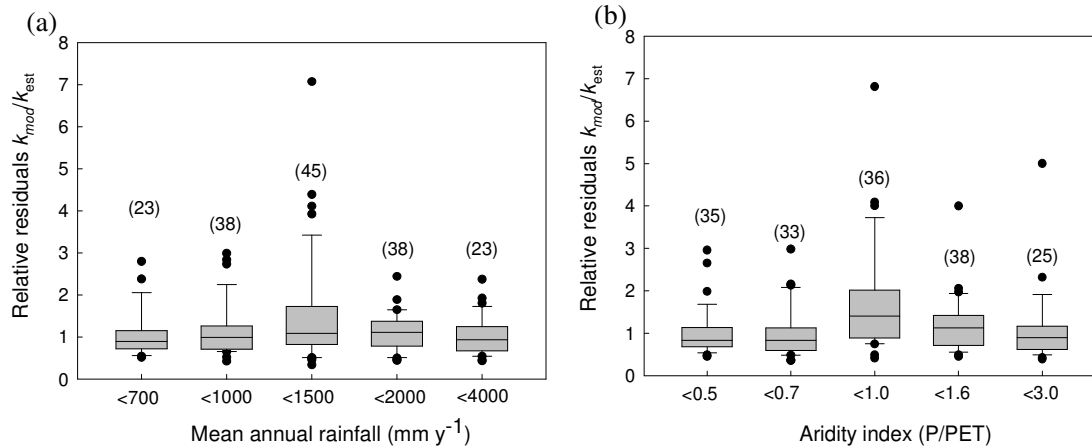


Fig. 6. Box and whiskers plot of relative residuals for exponential equations linking k_{bt} to (a) a range of mean annual rainfall classes (MAR). (b) Idem for aridity index (AI) range. The number in brackets is the sample size per range.

[Title Page](#)
[Abstract](#)
[Introduction](#)
[Conclusions](#)
[References](#)
[Tables](#)
[Figures](#)
[I◀](#)
[▶I](#)
[◀](#)
[▶](#)
[Back](#)
[Close](#)
[Full Screen / Esc](#)
[Printer-friendly Version](#)
[Interactive Discussion](#)


The role of climatic and terrain

J. L. Peña-Arancibia et al.

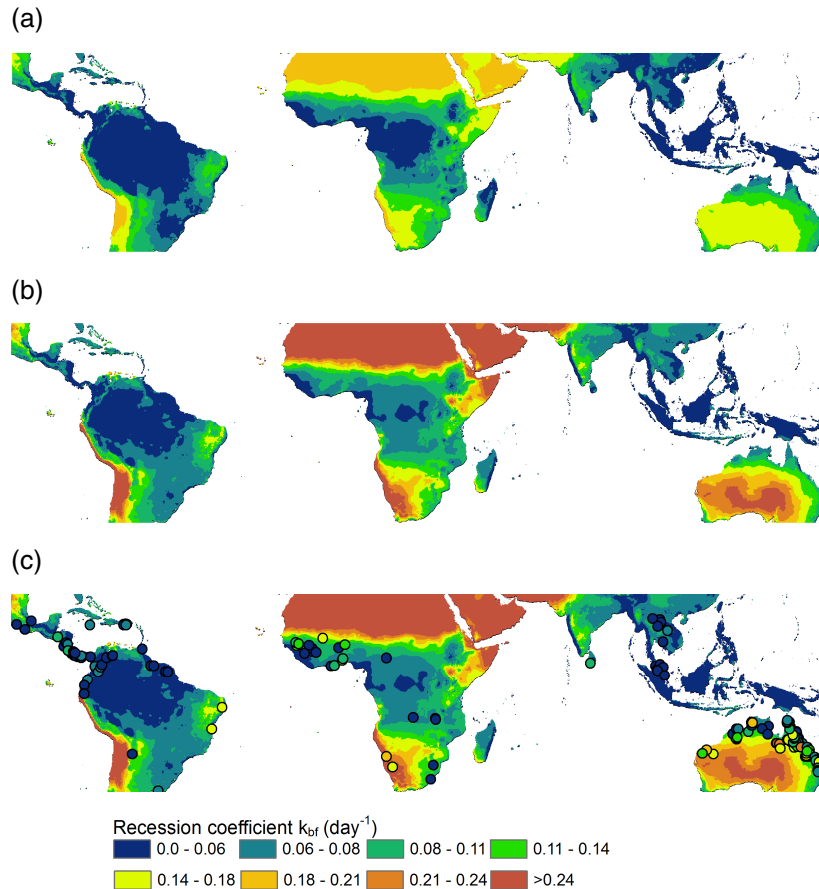


Fig. 7. Pan-tropical map of baseflow recession coefficient using the exponential regression equation and mean annual rainfall (MAR): **(a)** equation representing the lower and **(b)** upper bounds of the 95% confidence interval and **(c)** original regression equation. Symbol colours represent estimated k_{bf} values of the 161 catchments used in this study.

[Title Page](#)
[Abstract](#)
[Introduction](#)
[Conclusions](#)
[References](#)
[Tables](#)
[Figures](#)
[I◀](#)
[▶I](#)
[◀](#)
[▶](#)
[Back](#)
[Close](#)
[Full Screen / Esc](#)
[Printer-friendly Version](#)
[Interactive Discussion](#)
